Bulletin of the Seismological Society of America, Vol. 84, No. 4, pp. 1266–1271, August 1994

Routine Estimation of Earthquake Source Complexity: the 18 October 1992 Colombian Earthquake

by Charles J. Ammon,* Thorne Lay, Aaron A. Velasco, and John E. Vidale

Abstract We describe two methods, suitable for routine application to teleseismic recordings, that characterize the time history of seismic events. Stacking short-period signals from large regional arrays provides stable estimates of high-frequency radiation from the source, and an empirical Green's function deconvolution procedure extracts reliable, broadband time functions suitable for analysis of faulting complexity and the spatio-temporal extent of rupture. Combined, these procedures characterize the source radiation of large events ($M_S > 7$) between 200- and 0.5-sec periods.

Introduction

Routine estimation of earthquake source parameters has played an important role in the development of seismology. The construction of global and regional earthquake location and magnitude catalogs through routine processing over the last 80 yr has resulted in fundamental contributions to the development of global and regional tectonics. Over the last decade, researchers at Harvard (e.g., Dziewonski and Woodhouse, 1983) have constructed a catalog of centroid moment tensor (CMT) source models for moderate to large earthquakes, which now contains solutions for more than 10,000 events between 1977 and 1992. This compilation of first-order earthquake faulting parameters is an important facet of geological research. With the location, magnitude, and gross faulting mechanism of all moderate and large earthquakes now being established on a routine basis, and the near real-time availability of extensive high-quality digital seismic data, we now have an opportunity to develop new seismic reconnaissance tools.

An important aspect of large ($M_S > 7$) earthquakes that is desirable to routinely characterize is the source time function. The source time function contains information about the space-time history of the slip function on the fault. The CMT parameterization assumes the time history of faulting to be a box-car function, a reasonable approximation for the long-period radiation of moderate earthquakes, but often an inadequate parameterization for larger, complicated events. Much effort has already been invested in estimating time histories of faulting for specific events of interest, and high-resolution waveform inversion studies continue. For large events, this is often a tedious, and sometimes ambiguous, procedure, and there are commonly discrepancies in results between detailed investigations caused by unaccounted for structural effects. We focus here on the estimation of robust, first-order time function characteristics (duration, roughness, symmetry or asymmetry) of large ruptures using simple techniques that intrinsically suppress structural effects, yet can be applied routinely with a minimum investment of seismological research resources.

We describe two methods suitable for routine teleseismic wave application that can help characterize the time history of seismic events. Our application is to a pair of interesting, complex events that occurred in Colombia in 1992, temporally linked to the eruption of a mud volcano that killed several people. First, we illustrate the potential of large, short-period seismic arrays such as CALNET to provide stable estimates of the short-period radiation from the source region. Second, we exploit the expanding on-line broadband seismic data available at the Incorporated Research Institutions for Seismology (IRIS) Data Management System (DMS) and an empirical Green's function (EGF) technique to illustrate the potential for accurate and routine estimation of broadband (200 to 10 sec) source time functions of large earthquakes. Combined, these two techniques provide a characterization of the spatio-temporal seismic energy release between periods of 200 to 0.5 sec. The EGF approach requires little preprocessing and can be performed within hours after a major seismic event (Ammon *et al.*, 1993). Short-period array beamforming could also be completed within minutes after an earthquake, although at present, more time is necessary to access the data.

*Present address: Saint Louis University, Saint Louis, Missouri.

Table 1
Source Parameters*

Date	Time	Latitude	Longitude	Depth	M_S	M_w	% CLVD
10/17/92	08:32:40	6.836° N	76.873° W	10	6.6	6.7	80
10/18/92	15:11:59	7.067° N	76.870° W	10	7.2	7.2	72

*Location and M_S from NEIC Quick Epicenter Determination listing; M_w and % CLVD from Harvard

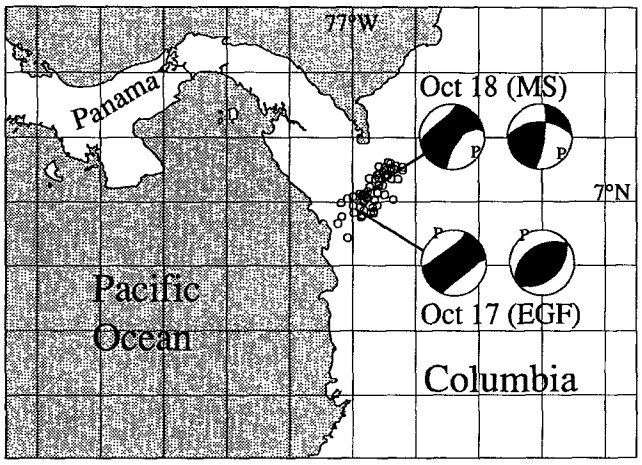

Figure 1. Locations and "quick" Harvard CMT solutions for the 17 and 18 October 1992 Colombian earthquakes. The mechanism on the left is the full moment tensor, the associated best double couple is on the right. Earthquakes reported in the QED listings between 17 October and 31 December 1992 are shown (circles). Grid spacing is 1°.

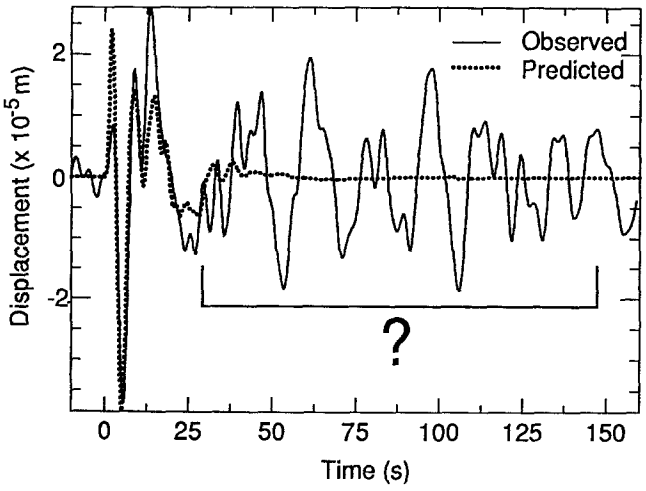

Figure 2. Comparison of the observed broadband P-wave displacement for the 17 October event recorded at COL (solid line) with a synthetic (dashed line). A source depth of 10 km and the CMT best double-couple mechanism were used to construct the synthetic. The complex coda is not explained by this model.

The October 1992 Colombian Earthquakes

To illustrate these procedures, we examine two earthquakes that occurred in northwestern Colombia in October of 1992. Both earthquakes are described by similar CMT moment tensors with large non-double-couple components (e.g., Frohlich *et al.*, 1989), but significantly different best double-couple mechanisms (Table 1, Fig. 1). However, in this case, the differences in the best double-couple mechanisms are not significant; at longer periods, the waveforms for both events are similar in appearance at a set of well-distributed stations. This waveform similarity indicates that the events actually had a similar focal mechanism. We begin with a qualitative analysis of the source complexity using P waveforms and then move on to a quantitative analysis using source time functions estimated from surface waves and P waves. We show that the 18 October event is a composite of three subevents; the first two occurred within 30 sec of the onset of rupture, and the third occurred approximately 100 sec later and could be considered an early aftershock. Each of the subevents is well described by a single pulse and little moment release occurred between the second and third subevents.

Source/Structure Complexity

Teleseismic broadband P waveforms for both Colombian events have a long duration of large-amplitude ground motion (Fig. 2), indicative of either source rupture complexity or near-source velocity structure complexity. The broadband source function analysis we employ requires *a priori* information on the location and depth of the event of interest. The depth of the 17 October event was fixed at 15 km by the Harvard group (Ekström, personal comm.), while the NEIC Quick Epicenter Determination (QED) depth estimate is 10 km. To confirm the shallow depths of the events, we compute synthetic seismograms using a one-layer, 30-km-thick crust, roughly consistent with crustal thickness estimates for the source region (e.g., Case *et al.*, 1990). We generate the synthetic seismograms using a propagator matrix technique to insure that all multiples near the source are included in the synthetic. We use the best double-couple estimate from the CMT inversion for the 17 October earthquake to compute the expected ground displacement. Figure 2 shows the fit of this model to the

displacements observed at station COL, College, Alaska ($\Delta = 76°$). The fit is reasonable, with the alignment of the depth phases indicating that the early moment release is located near 10-km depth.

Note the large amplitude arrivals between 40 to 160 sec after the *P* onset on the observed waveform at COL. These phases arrive well after the end of ground motion predicted by the synthetic seismogram. No major seismic phases are expected during this interval (*PcP* arrives near 12 sec, *PP* arrives near 160 sec). In Figure 3 we compare broadband and high-frequency *P*-wave observations observed in central California for the 17 October and 18 October events. The broadband recordings are from station BKS, Berkeley, California ($\Delta = 51°$), the high-frequency recordings are beamforms from more than 103 (17 October) and 147 (18 October) stations of the CALNET array. By stacking the short-period signals, local site effects are suppressed, and the common source-related signal is isolated. This stacking can now be performed routinely to characterize the high-frequency radiation from sources (e.g., Vidale and Houston, 1993) using telemetered short-period arrays around the world.

Large-amplitude secondary arrivals are visible on the BKS records for both events, with similar reverberations from 30 to 100 sec. These arrivals are similar to those on the COL waveform, indicating an origin near the source. These arrivals are not present in the frequency range 0.25 to 4 Hz, although strong high-frequency radiation from the first 20 to 30 sec is clear. Thus, if these later arrivals originate from a source process, it must be fundamentally different in frequency content than that which produced the initial energy and both earthquakes must have similar complex processes. A more likely origin for these waves is scattering of surface-to-body waves in the immediate vicinity of the sources, which will be similar for nearby events. The complexity of the broadband waveforms precludes standard source function inversions of these records, due to what we interpret to be the inadequacy of conventional plane layered Green's functions for a simple crustal model. How then can the source process of the larger event be reliably inferred without an extensive effort to model the near-source velocity structure?

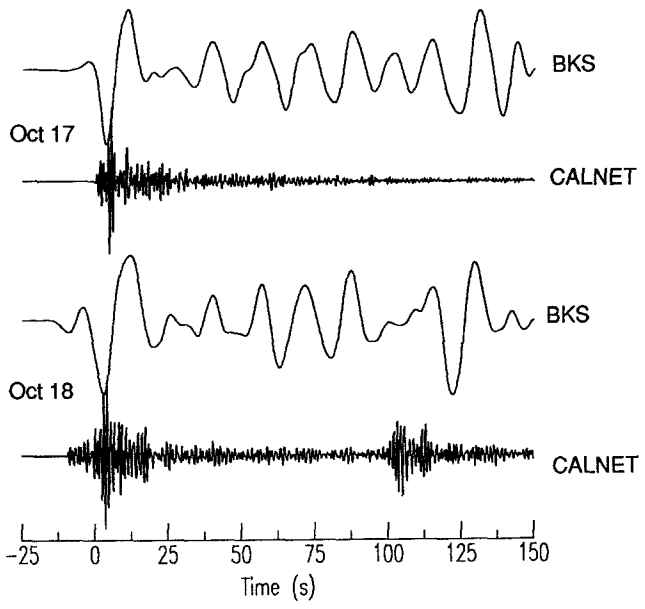

Figure 3. Comparison of the broadband *P*-wave ground velocities recorded at BKS and the high-frequency CALNET stacks for the two Colombian events. Each trace has been normalized to unity amplitude, the broadband waveforms have been low-pass filtered below 10-sec period.

Rupture Complexity of the 18 October Event

The 18 October event shows evidence of complexity in both the broadband *P* waves and the short-period CALNET stacks. In many of the 18 October broadband *P* waveforms, the initial polarity of the emergent waveform is opposite to that of the 17 October event but the subsequent large amplitudes in the waveform are very similar to the 17 October event for over 100 sec of ground motions. We conclude that the 18 October event began with a small subevent with a different mechanism than the dominant subevent, which occurred about 10 sec later. On the short-period CALNET stacks (Fig. 3), the 18 October event is also seen to have a clear high-frequency subevent (or aftershock) about 110 sec after the onset of motion with little high-frequency radiation between 50 and 110 sec. Near this time, the broadband waveform begins to differ from that of the 17 October event. This concordance of short- and long-period energy release is similar to the observations of Houston and Kanamori (1986).

The complexity of the near-source structure makes a quantitative analysis of the time history of the faulting using synthetic seismogram based approaches difficult, if not impossible. To account for the effects of this structure, we use an EGF approach to isolate the source time functions from both body and surface waves. This EGF approach was introduced by Ammon *et al.* (1993) in an analysis of the Landers and Cape Mendocino earthquakes of 1992, and is described in detail by Velasco *et al.* (1994). We obtain recordings from 13 seismic stations with good azimuthal distribution about the source and real-time access capability, stored on-line at the IRIS Data Management System. We examine Rayleigh, Love, and *P* waves from 13 stations and obtain 40 stable estimates of the relative source time function (RSTF) by deconvolving the seismograms for the mainshock (18 October) by the respective seismograms for the EGF (17 October). We consider the 17 October event to be a suitable EGF because its moment tensor and principal waveforms are similar to those of the 18 October event. Our procedure requires the availability of the CMT solutions,

which are routinely available within a few hours of large events.

The deconvolutions are performed in the frequency domain using a water-level method (Ammon *et al.*, 1993). For the surface waves, good signal-to-noise energy is observed over a large bandwidth (200 to 10 sec), and the deconvolutions are stable except near the radiation pattern nodes. The body waves have less long-period signal than the surface waves, but more short-period information. All of the RSTF's contain a large pulse of moment release followed by an impulsive event, approximately one-third as large, about 90 sec later (Fig. 4). The stable relative amplitude of the later pulse suggests that it has the same mechanism as the main pulse and the 17 October EGF. The main subevent occurs about 10 sec after the onset of motion. In those first 10 sec, a smaller subevent is observable on many, but not all, of the RSTF's. This pulse has polarity reversals for certain stations, supporting the notion that the first subevent has a slightly different mechanism than the EGF and the idea that it is different from the subsequent two pulses of the 18 October event. Our procedure does not readily establish the mechanism of the first subevent, although in some cases changes in mechanisms can be fully quantified (Ammon *et al.*, 1993).

We can quantify the locations and timing of the subevents found in the RSTF's because they are so impulsive in nature. We use a simple, relative-location method often used in body-wave analyses of large earthquakes (e.g., Hirasawa, 1965; Schwartz and Ruff, 1985) to estimate the location of the 18 October subevents relative to the primary moment release of the EGF. We present the results of the directivity analysis for the largest subevent of the 18 October event in Figure 5. The squares represent the time of the peak amplitude for the subevent (the centroid of the subevent) referenced to the EGF centroid. The linear correlation coefficient is 0.96, indicative of a very consistent set of observations and a good relative location of the centroid of this subevent. We attain a wide sampling of the directivity parameter by including deconvolutions for both body and surface waves.

We summarize the locations of the three subevents in Table 2 and Figure 6. The 18 October event began with a small event, with a different mechanism from the subsequent rupture, about 20 km south of the 17 October event. About 5 sec later, the largest subevent occurred, at almost the same location, with a mechanism similar

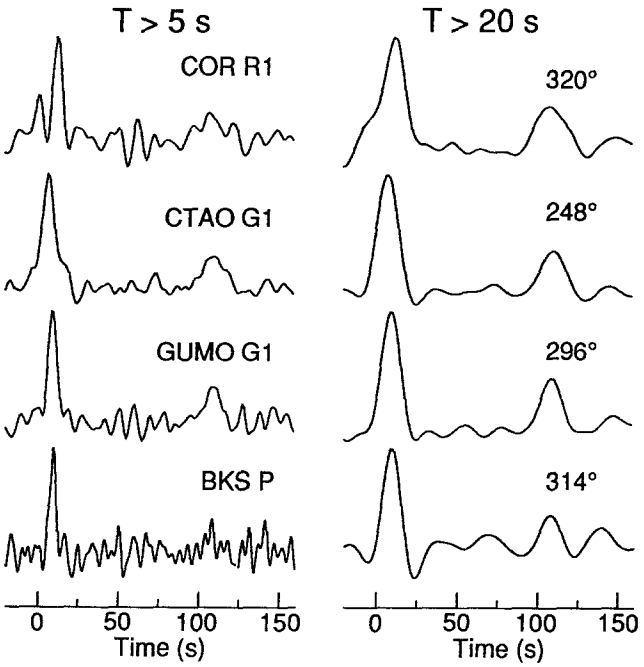

Figure 4. Estimated relative source time functions for the 18 October event determined by using the 17 October event as an empirical Green's function. The station names and phases used in the deconvolutions are shown. Left column: results low-pass filtered to include periods below 5 sec (zero-phase, four-pole Butterworth filter). Right column: results low-pass filtered below 20 sec.

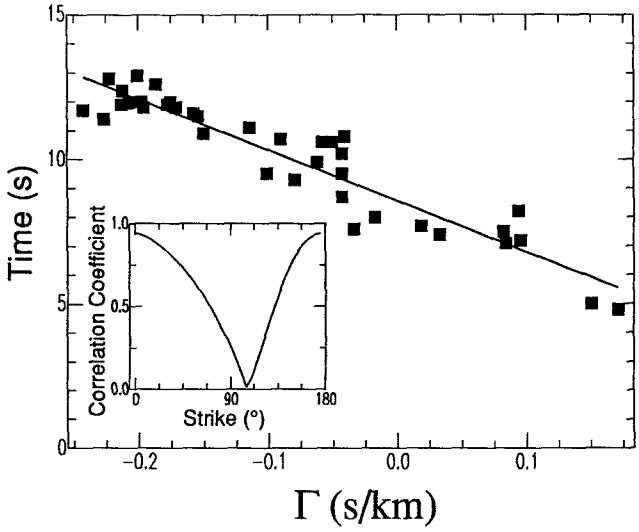

Figure 5. Directivity calculation for the second subevent of the 18 October event. The relative location is estimated by performing a grid search over the azimuth of a line connecting the EGF and mainshock subevent (inset) and computing the least-squares fit to the resulting linear relationship between the directivity parameter, Γ, and the observed time of the subevent on all the RSTF's. $\Gamma = \cos\theta/c$, where θ is the relative azimuth between the EGF and the subevent, and c is the phase velocity of the wave (4.38 km/sec for Love, 3.85 km/sec for Rayleigh, $(dT/d\Delta)^{-1}$ for body waves). Squares show measured times for the peak amplitude (centroid) of the subevent relative to the centroid of the 17 October event; the solid line shows the least-squares regression line. The inset shows the linear correlation coefficient as a function of azimuth. The highest correlation (0.96) occurs at an azimuth of 180°.

Table 2
Directivity Results

Subevent	Distance (km)	Azimuth (°)	Delay (sec)	Correlation Coefficient
1	18	175	−3	0.80
2	17	180	9	0.96
3	6	25	110	0.50

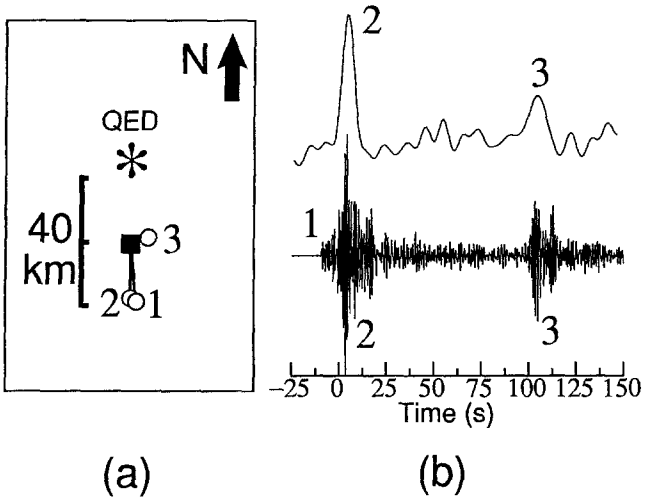

Figure 6. (a) Locations of the three subevents of the 18 October rupture relative to the NEIC-QED location for the 17 October event (square). The asterisk identifies the NEIC-QED location for the 18 October event. (b) Comparison of the estimated time function at GUMO (upper) and the CALNET short-period waveform stack (lower). Subevents are labeled on each waveform. The first subevent, not observed on the GUMO Love waves, is likely nodal in this direction.

to the 17 October event. Approximately 100 sec later, very near the location of the 17 October event, another subevent with a similar mechanism to the 17 October event occurred. Although the azimuth of this third subevent is not well constrained by the location procedure (note the small correlation coefficient in Table 2), the small moveout of the subevent observed on the RSTF's requires that the distance between the centroids of this subevent and the EGF be approximately 0 to 10 km. Between the second and third subevents, no detectable moment release occurred and the third subevent can be considered an early, large aftershock. The relative locations of the subevents suggests that the mainshock occurred along a north–south-striking trend. However, the trend of the aftershocks suggests that a northeast–southwest oriented structure is involved. Since we found little evidence for slip between the early and later subevents, it is possible that the events occurred along subparallel, northeast/southwest-trending faults, offset from each other about 20 km in a north–south direction.

The non-double-couple nature of the 18 October CMT solution could be partly attributable to the subevent complexity. However, since the 17 October event was found to have a similar large non-double-couple component, apparently because of propagation effects, the larger event is probably also affected. While the original records are very complex, the deconvolutions in Figure 4 are quite simple to interpret, reflecting the successful removal of propagation effects. The multiple subevent nature of the mainshock rupture is readily revealed by our deconvolution and directivity procedure. While it may be that after substantial effort to develop appropriate three-dimensional Green's functions for the mainshock, a comparable characterization of the rupture process could be obtained by waveform inversion methods, our procedure retrieved these basic characteristics within a few hours, dependent only upon moment-tensor solutions and the availability of suitable records for a nearby EGF. The accumulating data in the IRIS DMS ensure that many large events will have a suitable prior event available for use in comparable analyses.

Discussion

Analysis of complex earthquakes often requires a large amount of seismological research resources. We have presented two simple approaches that can be used to estimate the first-order properties of seismic rupture source functions in a routine fashion. Short-period array stacking can be applied to practically all events, although the limited bandwidth of the stack limits the utility of the resulting waveforms. The empirical Green's function approach also has limitations because of the requirement of a nearby, similar mechanism event with corresponding path coverage. However, the increasing data base maintained by IRIS, and the common occurrence of aftershocks following a large event, makes this approach viable for many large earthquakes (Velasco *et al.*, 1994). Our deconvolution procedure builds naturally on the well-developed capabilities for rapidly obtaining point-source moment-tensor solutions. The simplicity of our techniques offers the promise of routine processing of most large events, and the large bandwidth (0.25 to 200 sec) allows the near real-time identification and location of interesting phenomena such as multiple events and slow earthquakes. In some cases this will have practical use for disaster response, such as characterizing tsunamigenic ruptures, locating energetic bursts of moment release, or identifying the actual orientation of the fault plane.

Acknowledgments

We thank the IRIS Data Management System for its rapid collection and open access to global digital data required for this type of work. Gorän Ekström provided us with information about the Harvard CMT

solutions for the Colombian events. This work was supported by NSF Grant Number EAR-9017767. Research at UCSC on near real-time analysis of large earthquakes is also supported by a grant from the Southern California Earthquake Center and the W. M. Keck Foundation. Contribution number 201 from the Institute of Tectonics and C. F. Richter Seismological Laboratory, University of California, Santa Cruz.

References

Ammon, C. J., A. A. Velasco, and T. Lay (1993). Rapid estimation of rupture directivity: application to the 1992 Landers (M_s = 7.4) and Cape Mendocino (M_s = 7.2) California earthquakes, *Geophys. Res. Lett.* **20**, 97–100.

Case, J. E., W. D. MacDonald, and P. J. Fox (1990). Caribbean crustal provinces; seismic and gravity evidence, in *The Caribbean Region, The Geology of North America*, G. Dengo and J. E. Case (Editors), Geological Society of America, Boulder, Colorado, 15–36.

Dziewonski, A. M. and J. H. Woodhouse (1983). An experiment in systematic study of global seismicity: centroid-moment tensor solutions for 201 moderate and large earthquakes of 1981, *J. Geophys. Res.* **88**, 3247–3271.

Frolich, C., M. A. Riedesel, and K. D. Apperson (1989). Note concerning possible mechanisms for non-double-couple earthquake sources, *Geophys Res. Lett.* **16**, 523–526.

Hirasawa, T. (1965). Source mechanism of the Niigata earthquake of June 16, 1964, as derived from body waves, *J. Phys. Earth* **13**, 35–66.

Houston, H. and H. Kanamori (1986). Source spectra of great earthquakes: teleseismic constraints on rupture process and strong ground motion, *Bull. Seism. Soc. Am.* **76**, 19–42.

Schwartz, S. Y. and L. J. Ruff (1985). The 1968 Tokachi-Oki and the 1969 Kurile Islands earthquakes: variability in the rupture process, *J. Geophys. Res.* **90**, 8613–8626.

Velasco, A. A., C. J. Ammon, and T. Lay (1994). Empirical Green function deconvolution of broadband surface waves: rupture directivity of the 1992 Landers, California (M_w = 7.3) earthquake, *Bull. Seism. Soc. Am.* (in press).

Vidale, J. E. and H. Houston (1993). The depth dependence of earthquake duration and implications for rupture mechanisms, *Nature* **365**, 45–47.

University of California, Santa Cruz
Santa Cruz, California 95064
(C.J.A., T.L., A.A.V.)

U.S. Geological Survey
Menlo Park, California 94025
(J.E.V.)

Manuscript received 4 March 1993.